CHALMERS
UNIVERSITY OF TECHNOLOGY

Oxidized xylan additive for nanocellulose films – A swelling modifier

Downloaded from: https://research.chalmers.se, 2024-04-23 17:46 UTC

Citation for the original published paper (version of record):
Palasingh, C., Ström, A., Amer, H. et al (2021). Oxidized xylan additive for nanocellulose films – A swelling modifier. International Journal of Biological Macromolecules, 180: 753-759.
http://dx.doi.org/10.1016/j.ijbiomac.2021.03.062

N.B. When citing this work, cite the original published paper.

research.chalmers.se offers the possibility of retrieving research publications produced at Chalmers University of Technology.
It covers all kind of research output: articles, dissertations, conference papers, reports etc. since 2004.
research.chalmers.se is administrated and maintained by Chalmers Library

(article starts on next page)

International Journal of Biological Macromolecules 180 (2021) 753–759

Contents lists available at ScienceDirect

International Journal of Biological Macromolecules

journal homepage: http://www.elsevier.com/locate/ijbiomac

Oxidized xylan additive for nanocellulose films – A swelling modifier

Chonnipa Palasingh [a], Anna Ström [a], Hassan Amer [b,c], Tiina Nypelö [a,d,*]

[a] Applied Chemistry, Department of Chemistry and Chemical Engineering, Chalmers University of Technology, 41296 Gothenburg, Sweden
[b] Institute of Chemistry of Renewable Resources, Department of Chemistry, University of Natural Resources and Life Sciences, Tulln, Konrad-Lorenz Straße 24, 3430 Tulln, Austria
[c] Department of Natural and Microbial Products Chemistry, National Research Centre, 33 AlBohous St., Dokki, Giza, Egypt
[d] Wallenberg Wood Science Center, Chalmers University of Technology, Gothenburg, Sweden

ARTICLE INFO

Article history:
Received 13 December 2020
Received in revised form 5 March 2021
Accepted 12 March 2021
Available online 13 March 2021

Keywords:
Wood components
Renewable materials
Sustainable engineering

ABSTRACT

Polymeric wood hemicelluloses are depicted to join cellulose, starch and chitosan as key polysaccharides for sustainable materials engineering. However, the approaches to incorporate hemicelluloses in emerging bio-based products are challenged by lack of specific benefit, other than the biomass-origin, although their utilization would contribute to sustainable material use since they currently are a side stream that is not valorized. Here we demonstrate wood-xylans as swelling modifiers for neutral and charged nanocellulose films that have already entered the sustainable packaging applications, however, suffer from humidity sensitivity. The oxidative modification is used to modulate the water-solubility of xylan and hence enable adsorption in an aqueous environment. A high molecular weight grade, hence less water-soluble, adsorbed preferentially on the neutral surface while the adsorbed amount on a negatively charged surface was independent of the molecular weight, and hence, solubility. The adsorption of the oxidized xylans on a neutral cellulose surface resulted in an increase in the amount of water in the film while on the negatively charged cellulose the total amount of water decreased. The finding of synergy of two hygroscopic materials to decrease swelling in hydrophilic bio-polymer films demonstrates the oxidized macromolecule xylan as structurally functional component in emerging cellulose products.

© 2021 The Authors. Published by Elsevier B.V. This is an open access article under the CC BY license (http://creativecommons.org/licenses/by/4.0/).

1. Introduction

The global increase in the consumption of plastic materials and dispose rate has created a need to transfer from non-renewable feedstock to renewable ones, without compromising food supply or land use. Most of the consumable plastics are made from non-renewable fossil fuels, while only 2% are made from renewable materials [1]. Cellulose is composed of β-1,4-glycosidic linked glucose units and arranged in plant cell wall into microfibrils with dimensions in the order of nano to micrometer [2]. The cellulose microfibrils can contribute to a new generation of packaging material [3–6]. However, the abundant hydroxyl groups of the cellulose lead to interaction with water and make the material sensitive to humidity [7,8].

Hemicelluloses in wood are bound to cellulose fibrils and are present in a majority of cellulose products as well [9]. Hardwood hemicelluloses provide xylans as dominant component while softwood hemicelluloses are rich in glucomannans. Xylan, which is the focus of this study, is composed of β-1,4-linked xylose backbone that can carry substituting glucuronic acid, arabinose, galactose or acetyl units [10]. The hemicelluloses bound to cellulose have been reported to act as hydration modifiers for cellulose nanofibers and contribute to stability in a range of pH and salt concentrations [11]. There are also implications of hemicelluloses as friction modifiers for cellulose surfaces [12]. Adsorptive modification of cellulose substrates has been reported by xylans [13], acetylated xylans [14], arabinoxylans [15–17], xyloglucans [18,19], and glucurunoxylans [20,21]. Interaction of xylan and cellulose in plant cell wall have shown to occur through a twofold helical screw conformation, promoting hydrogen bonding, while xylan conformation in solution is a threefold helical screw [22–24]. An adsorbed xylan tends to stretch to cover unoccupied regions and free adsorbent surface already at low concentration. Loop and tail conformation of the xylan was found more often with increasing concentration [19]. Linder et al. [25] suggested xylan to aggregate in the solution before being adsorbed on cellulose surface. The tendency of xylan aggregation in solution has been acknowledged by others as well [26,27]. Despite the increasing interest towards the intrinsic properties of wood hemicelluloses, there are few demonstrations of their use in materials engineering, for example in packaging [26,28,29].

In this study, wood-based xylans were incorporated into cellulose films with the aim to decrease the film hygroscopicity. Film hygroscopicity was aimed to be reduced via increasing the linkages between the macromolecules on the expense of those with water. Periodate oxidation was used to increase xylan water-solubility via cleavage between C2 and C3 of xylose backbone and alteration of the molecular

* Corresponding author at: Applied Chemistry, Department of Chemistry and Chemical Engineering, Chalmers University of Technology, 41296 Gothenburg, Sweden.
E-mail address: tiina.nypelo@chalmers.se (T. Nypelö).

https://doi.org/10.1016/j.ijbiomac.2021.03.062
0141-8130/© 2021 The Authors. Published by Elsevier B.V. This is an open access article under the CC BY license (http://creativecommons.org/licenses/by/4.0/).

conformation into poly(2,6-dihydroxy-3-methoxy-5-methyl-3,5-diyl-1,4-dioxane) [30]. The water-solubility was sought to enable cellulose film modification via adsorption in water that is an important solvent system for polysaccharide engineering. Adsorption of oxidized xylans on cellulose film is elaborated with quartz crystal microbalance with dissipation monitoring (QCM-D) and surface plasmon resonance (SPR) with focus on revealing the changes in film swelling upon introduction of the hemicellulose additives. Our findings of increasing macromolecular wood-xylan solubility, of incorporating it to emerging cellulose products and identifying a structural functionality contribute towards new class of biological macromolecules for sustainable engineering.

2. Experimental

2.1. Materials

$NaIO_4$, TEMPO, NaBr, PEI (branched, average M_w 25,000 g/mol) and NaClO were purchased from Merck and used as received. Cellulose nanofibers (CNF, plural CNFs) from softwood kraft pulp was a product of Innventia, Sweden. Relative carbohydrate composition of CNFs was 97 ± 0.5% glucose, 2 ± 0.5% xylose and 1 ± 0.1% mannose using acid hydrolysis and high performance anion exchange chromatography (HPAEC). Acid soluble lignin content was 0.9 ± 0.2% determined via measurement of absorbance at 205 nm utilizing the hydrolysate that was used in the relative carbohydrate composition analysis. Xylans from kraft pulping were extracted from beech wood (see details of this grade in Amer et al. [30]) and birch wood. According to gel permeation chromatography in DMSO/LiBr, the starting xylan from beech wood was 7,700 g/mol and xylan from birch wood had molecular weight of 31,000 g/mol. After modification, the molecular weight of the oxidized xylan was 5,100 g/mol and 13,000 g/mol, respectively. Hereafter, the oxidized xylan from beech wood will be referred to as low molecular weight oxidized xylan (LX) and oxidized xylan from birch wood as high molecular weight oxidized xylan (HX). The degree of oxidation was determined by measuring UV absorbance at 290 nm during oxidation [31].

TEMPO-oxidized cellulose nanofibers (TCNFs) were prepared according to Saito et al. [32]. In short, a suspension containing 1 g of CNFs, 0.1 mmol of TEMPO and 1 mmol of NaBr in 100 ml water was prepared. Then 3.8 mmol of 12% NaClO solution was added and pH was adjusted to 10. The suspension was stirred at room temperature and 0.5 M NaOH was added dropwise to maintain pH at 10 until no further change took place. The product was dialyzed, the dry matter determined using an infrared dryer (LJ16, Mettler Toledo) and charge using particle charge detector (PCD 02, Mütek).

2.2. Carbohydrate composition

Xylans and oxidized xylans were hydrolyzed with 72% sulfuric acid at 125 °C for 1 h [33]. The hydrolyzed xylans were filtrated through 0.2 μm nylon filter. Fucose was used as internal standard. The xylans were analyzed with high performance anion exchange chromatography with pulsed amperometric detection (HPAEC-PAD) using Dionex ICS 3000 ion chromatography system equipped with a CarboPac PA1 analytical column.

2.3. Dynamic light scattering (DLS)

Zetasizer (Zetasizer nano ZS90, Malvern) was used for determining hydrodynamic diameter of the oxidized xylan solutions. The xylans were dissolved in phosphate buffer solution (PBS, pH 7.4, 100 mM NaCl) overnight and were filtrated through 0.45 μm nylon filter. Each measurement is an average of 3 measurements. The measurements were performed at 22 °C and with 120 s equilibration time. Refractive index of the oxidized xylan was determined using a refractometer (Abbemat 550, Anton Paar). Hydrodynamic diameter (d_H) was calculated form a transitional diffusion coefficient (D) by using Stokes-Einstein equation (Eq. (1))

$$d_H = \frac{kT}{3\pi\eta D} \tag{1}$$

where k is Boltzmann's constant, T is absolute temperature and η is viscosity. A number distribution and diffusion coefficient were determined from autocorrelation function.

2.4. Film preparation

Thin films for adsorption experiments were prepared by spin coating on the QCM-D and SPR silicon sensors. A PEI anchoring layer was electrostatically adsorbed on a sensor surface using 1.6 g/l of PEI solution. The CNFs and TCNFs were diluted to 1.7 g/l. These suspensions were sonicated with ultrasound (Vibra-Cell, Sonics & Materials, Inc.) in ice bath for 5 min and centrifuged at 6,000 rpm for 40 min (ultracentrifuge Optima XL-100K, Beckman Coulter). A supernatant was used for spin coating (Spin 150, SPS) two layers at 3,000 rpm for 60 s. The films were dried in an oven at 80 °C for 10 min to ensure nanofiber attachment.

2.5. Quartz crystal microbalance with dissipation

The experiments were performed using QCM-D (Q-Sense E4, Biolin Scientific) and silicon coated sensors (QSX303, Biolin Scientific). Oxidized xylan grades were dissolved in the PBS buffer (pH 7.4, 100 mM NaCl) at concentration of 0.01 wt%. Experiments were performed with 100 μl/min flow rate at 22 °C for 2 h.

The film thickness was analyzed according to Tammelin and coworkers [34] by recording the resonance frequency in air and stitching together the frequency of the films on the sensors before and after adsorption using QSoft and QTools softwares. Thickness (d) was calculated through mass change (Δm) according to Sauerbrey equation (Eqs. (2) and (3)):

$$\Delta m = -C\frac{\Delta f}{n} \tag{2}$$

$$d = \frac{\Delta m}{\rho} \tag{3}$$

where Δf is resonance frequency different, n is an overtone number and C is a sensitivity constant of sensor which is 0.177 mg/(Hz m^2), assuming density (ρ) of 1,500 kg/m^3.

An adsorbed mass was calculated according to Eq. (4) derived by Naderi and Claesson [35] from Johannsmann et al. [36]

$$\hat{m}^* = m^0\left(1 + \hat{J}(f)\frac{\rho f^2 d^2}{3}\right) \tag{4}$$

where $\left(\hat{m}^*\right)$ denotes an equivalent mass, $\hat{J}(f)$ stands for complex shear compliance, which is assumed as constant, ρ the density of the fluid, f the resonance frequency and d a thickness of the film. A true sensed mass (m^0), which is the adsorbed mass, is obtained from interception of linear fitting of plot of $\left(\hat{m}^*\right)$ against f^2.

Water content in the films was determined using H_2O/D_2O solvent exchange [37,38]. Water was introduced to QCM-D flow cell with 100 μl/min flow rate. After plateau in a baseline was obtained, water was exchanged with D_2O for 5 min before changed back to H_2O. Change in resonance frequency between H_2O and D_2O of bare sensor ($(\Delta f/n)_{bare}$) and cellulosic film ($(\Delta f/n)_{film}$) was recorded and Eqs. (5) and (6) were used to calculate the water

content of the film (Γ_{water}) through resonance frequency change $(\Delta f/n)_{water}$.

$$\left(\frac{\Delta f}{n}\right)_{water} = \frac{\left(\frac{\Delta f}{n}\right)_{film} - \left(\frac{\Delta f}{n}\right)_{bare}}{\left(\frac{\rho_{D_2O}}{\rho_{H_2O}}\right) - 1} \quad (5)$$

$$\Gamma_{water} = -C\left(\frac{\Delta f}{n}\right)_{water} \quad (6)$$

where ρ_{D_2O} and ρ_{H_2O} are the solvent densities, respectively.

2.6. Surface plasmon resonance

SPR Navi 220A (BioNavis Ltd.) was used and films were prepared on commercial SPR sensors with a SiO_2 surface (BioNavis Ltd.) were used for recording adsorption of oxidized xylans at 10 μl/min and otherwise with same conditions as the QCM-D analysis. Dry layer thickness was obtained through modeling of SPR data using Fresnel model [39]. Adsorbed mass was calculated through the modified De Feijter equation (Eq. (7)).

$$\Gamma = \frac{\Delta\Theta\ k\ d_p}{\frac{dn}{dc}} \quad (7)$$

where $\Delta\theta$ is the angular response of the surface plasmon resonance, k is a sensitivity constant of SPR, d_p is thickness of adsorbed layer and dn/dc is refractive index increment of oxidized xylan. For layer thinner than 100 nm, kd_p can be considered constant. The kd_p for 670 nm and 975 nm are 0.91×10^{-7} cm/° and 1.56×10^{-7} cm/°, respectively. The dn/dc of HX and LX in the buffer were estimated using a refractometer (Abbemat 550, Anton Paar), the values are 0.141, and 0.122 ml/g for HX and LX, respectively.

2.7. Atomic force microscope (AFM)

Topography of films on QCM-D sensors and SPR sensors was investigated with NTEGRA AFM (NT-MDT) with NSG01 tips with resonant frequency of 87–230 kHz and force constant of 1.45–15.1 N/m. Topography images of three positions or more on each specimen were recorded and processed using Gwyddion software.

3. Results and discussion

3.1. Oxidized xylans in solution

Periodate oxidation is a well-known modification for polysaccharides [40–42], and it is possible to oxidize xylan to a high degree, with proposed increased flexibility albeit reduced molecular weight [43], and increased reactivity to crosslinking [44]. Recycling of the periodate has been established [45] and leads to a decrease in the reagent consumption and hence cost and environmental burden of the modification step [46,47]. The non-oxidized HX and LX, composed of approximately 90 wt% of xylose with ≤2 wt% arabinose and glucose residues (Table 1), were both oxidized to 92% degree of oxidation, as detected by analysis of the oxidant consumption. The degree of oxidation was furthermore probed by determination of the relative carbohydrate composition of the oxidized grades (Table 1). The hydrolysis cleaves the oxidized rings leaving only the non-oxidized monosaccharides to be detected. The oxidation reduced the detected xylose monosaccharide by 93 wt% and 95 wt% for HX and LX, respectively, which supports degree of oxidation determined by the oxidant consumption. Hence, the two oxidized xylan grades that were used, HX and LX comprised of similar carbohydrate composition and a high degree of oxidation, leaving the molecular weight as the differentiating property.

A structure of aldehyde groups on oxidized xylan usually presents as an aldehyde in dry state, while it converts to a hydrated form in a presence of water (Fig. 1). The hydrated aldehydes can further form hemialdal structure by bridging two aldehyde groups with at least one in hydrated form on C2 and C3 of neighboring unit. As a result, oxidized polysaccharides are in an equilibrium of hydrated aldehyde form and hemialdal form in a solution [30,48].

DLS was used to evaluate the hydrodynamic diameter (d_H) of the oxidized xylans in the buffer solution. The d_H increased with the concentration of oxidized xylans independent of molecular weight (Fig. 2a and b). The mean average of d_H of HX and LX was approximately 3.6 nm and 0.6 nm for 0.01 wt% and 24.4 nm and 1.5 nm for 0.1 wt%, respectively. The shape of the correlation curve indicates higher polydispersity of LX grade (Supplementary information Fig. A1).

3.2. Adsorption of oxidized xylan on cellulose films

QCM-D is an acoustic method and the adsorbed mass is the sum of the absorbate and the solvent in the adsorbing film. The adsorbed mass calculated from the SPR is based on the refractive index increment (Eq. (7)) and enables quantification of the mass of the absorbent molecules only. Consequently, the adsorbed masses determined by SPR were lower than those determined by the QCM-D (Fig. 3).

The HX grade resulted in a larger adsorbed amount on the neutral CNF surface than the LX grade (Fig. 3). Kabel et al. [19] reported that high molecular weight xyloglucan adsorbed more on bacterial cellulose than lower molecular weight. The molecular weight of macromolecules affects their solubility as well as aggregation in a solution and contribute to the adsorption. The d_H of the HX increased by 6.8-fold while the increase in LX was 2.5-fold when increasing the concentration from 0.01 to 0.1 wt%. That is, the increase in concentration affects aggregation of HX to a larger extent than LX. This implies that the HX grade is less water-soluble compared to the LX and hence has a preference to the surface over the solvent. The chain length has also an entropic aspect to the adsorption. Even though, a surface has an equal affinity towards different chain lengths, entropy decreases to a larger extent with longer molecules which is preferable for the system [54].

The negative charges were introduced to the cellulose film by oxidation of the alcohols in the C6 position to carboxylate (TCNFs) and the initial charge of −35.51 μeq/g increased to −409.58 μeq/g. The presence of deprotonated carboxyl groups enhance the self-assembly of TCNFs [49] and can decrease the ionic attraction with adsorbed oxidized xylan. Indeed, the adsorbed amount based on the QCM-D of the HX was reduced compared to the adsorption on, the close to, neutral charged CNF film. The adsorbed amount with LX remained at a similar level as in the case of CNF films. An effect of adsorbate molecular weight was no longer pronounced. A competition between counter-ions and uncharged oxidized xylan segments for a space on the surface likely affected the adsorption in terms of balancing entropy gain form the adsorption and maintaining electroneutrality of the surface. The

Table 1
Relative carbohydrate composition of non-oxidized and oxidized xylans.

in wt%	Arabinose	Galactose	Glucose	Xylose	Mannose	Total carbohydrates
Non-oxidized HX	<1	0	<1	89	0	90
Non-oxidized LX	<1	0	2	89	0	91
Oxidized HX	<1	0	0	6	0	7
Oxidized LX	1	0	0	4	0	5

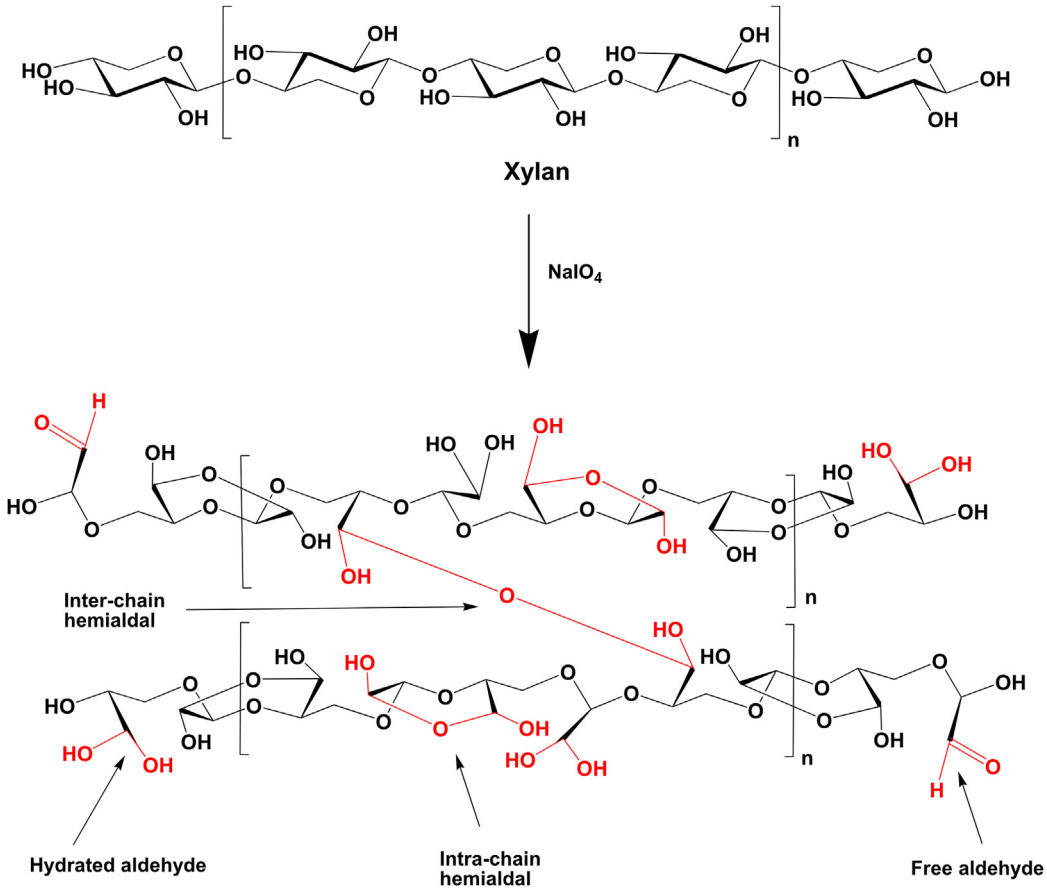

Fig. 1. Schematic presentation of xylan, oxidized with $NaIO_4$. The oxidation leads to an aldehyde functionality that converts into various forms in solution (denoted in red). The aldehydes hydrate in presence of water and can further form inter and intra-chain hemialdals.

introduction of the carboxylates should also increase the affinity between water and cellulose. The TCNF interface is hypothesized to contain more water than the CNF surface. This would inhibit the adsorption of molecules whose adsorption is driven by entropy gain due to lower solubility, such as the HX.

Only the QCM-D adsorption could be evaluated for the TCNF films because an extremely low amount of oxidized xylans were detected with SPR for the HX and it did not allow reliable modeling of the adsorbed mass. However, the mass detected implies that the adsorbed amount of the HX is low while dissipation level of 1.3×10^{-6} indicates that the deposited component has a pronounced viscous character further indicating that it is swollen. In the case of LX, the mass detected by SPR was in the same range as determined with QCM-D but with a high standard deviation.

The development of viscoelasticity of films during adsorption was revealed by contrasting the change in dissipation (ΔD) to the change in frequency (Δf) of the QCM-D (Fig. 4). The magnitude of negative frequency correlates with the amount of adsorbed mass. The increasing dissipation value indicates film viscoelastic property change. Increasing slope of the $\Delta D/\Delta f$ plot can indicate that more water binds to the surface

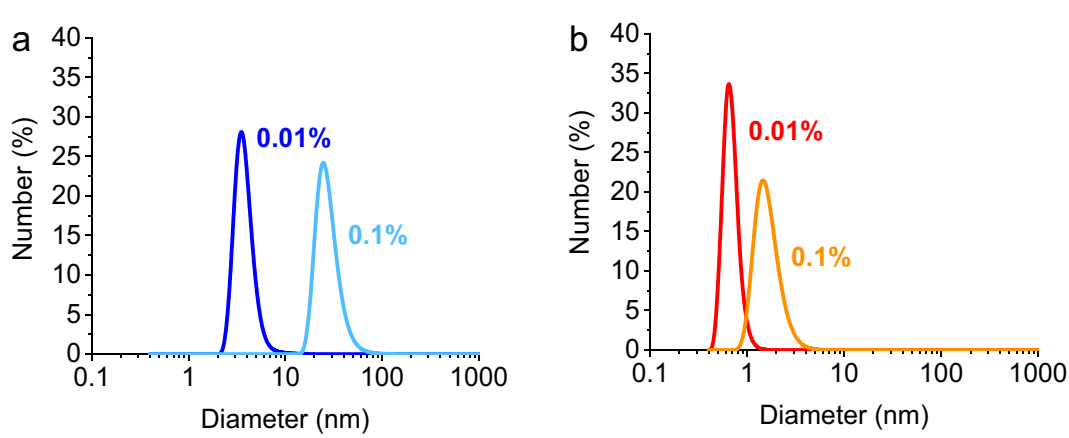

Fig. 2. Size distribution by number of HX (a) and LX (b) dispersed in PBS buffer at concentrations of 0.1 and 0.01 wt% determined in 22 °C .

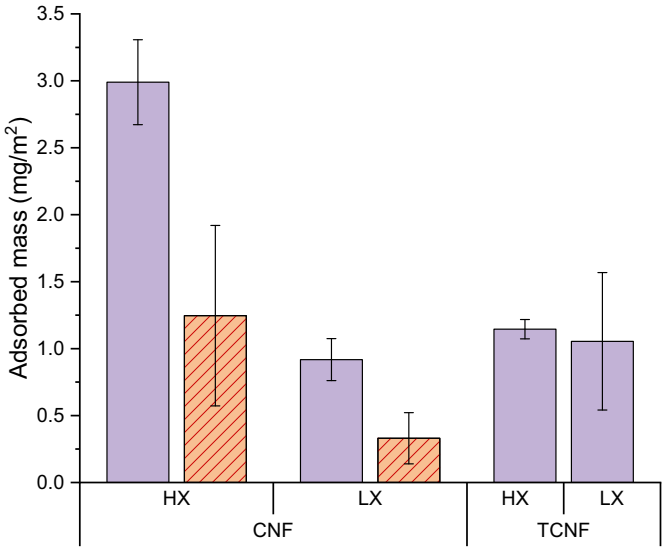

Fig. 3. Adsorbed mass of HX and LX on CNF and TCNF films using QCM-D (▨) and SPR (▨).

than adsorbate. The HX adsorption on CNF film was first characterized by a fast adsorption that is indicated by the reduced density of the measurement points recorded at a constant frequency. The mass and the dissipation increase linearly. The LX adsorption is slower, as indicated by the uniform density of the measurement points with increasing Δf. The lower slope indicates that the film is dominated by the elastic component compared to the case of HX, thus forming a denser structure. The DLS measurements revealed that the HX assemblies have a larger diameter of hydration in these conditions than the LX. The lowered ΔD/Δf slope of LX in comparison to HX is taken to support that observation and to indicate that the HX introduces more water to the system than LX.

In the case of adsorption on the TCNF film, the dissipation increases faster with respect to the mass than on the CNF substrate. This suggests that the adsorption of LX or HX on TCNFs leads to films containing more water, than those composed of LX or HX and CNFs. However, the ΔD/Δf curve of the LX adsorption on TCNFs reveals a change in the slope with higher rate of water uptake at the beginning than in the end. This tendency is opposite to the adsorption on CNFs where the increase is linear.

The kinetics of the adsorption over time is presented in Supplementary Information Fig. A2 with the minimum intensity angle shift during the adsorption in SPR. After the initial higher adsorption rate, the rate decreases. The adsorption does not reach a plateau within the 2-hour measurement time and manifests a slow adsorption of the oxidized xylans on the cellulose surfaces. We note that this was a general tendency for all the grades and relates to polydispersity of oxidized xylans. Polydisperse solutions take a longer time to reach a plateau in adsorption than monodisperse due to that small molecules diffuse to a surface faster and adsorb first after which the larger molecules eventually displace the smaller ones [54].

The CNF films were thicker than TCNF films in the dry state (Fig. 5). This results from the ionic repulsion between the like-charged TCNFs that leads to a better dispersed suspension [50] and thinner films. SPR analysis showed similar initial thickness of both films with less than 1 nm difference comparing to the values extracted from the QCM-D result presented in Fig. 5. In both cases, there was a slight increase in the film thickness after the adsorption of the oxidized xylans on the surface. However, even if the increase in mean values indicates a nominal increase in the layer thickness, analysis revealed no statistically significant change after the LX adsorption on both CNF and TCNF film.

The appearance of the films in AFM analysis was similar independent of adsorption or type of oxidized xylan (Supplementary Information file Fig. A3). Eronen et al. [51] reported similar results with arabinoxylans and xyloglucan adsorption on CNF films. There was no sign of hemicellulose moieties on the surface. These findings imply that the assemblies are either reorienting during adsorption or do not contribute enough to the film conformation to be detectable by AFM.

3.3. Water content in the films

A solvent exchange method utilizing the density difference of water and deuterated water [38] was employed to evaluate the water content in the neat CNF and TCNF films as well as after adsorption of HX and LX (Fig. 6). Kittle et al. [37] reported that water amount in cellulose films is proportional to film thickness. Since the thickness of the CNF and TCNF films was different, we have converted the water amount to a dry matter content by considering the initial film mass. The TCNF films contained more water (73%) than the CNF films (56%) as a result of charged TCNF network that promotes swelling [52]. Our findings comply to those of Kontturi et al. [53] who found that CNF thin film solid content in swollen state was below 50%.

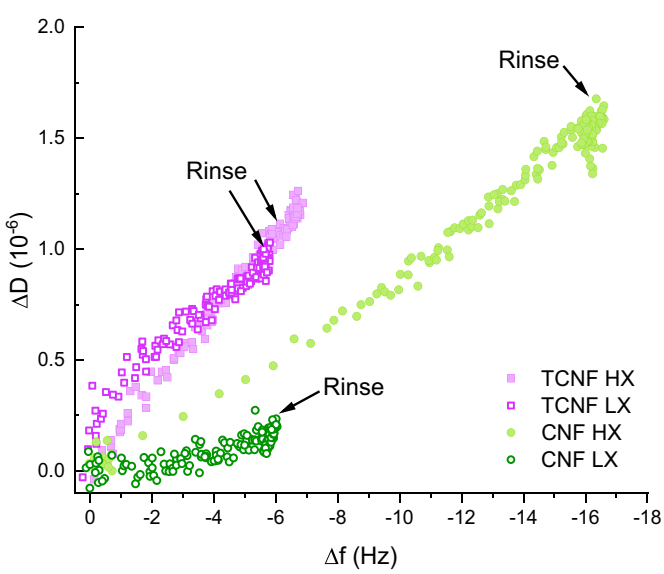

Fig. 4. Change in dissipation (ΔD) versus change in frequency (Δf) of 7th overtone upon adsorption of HX and LX on CNF and TCNF films.

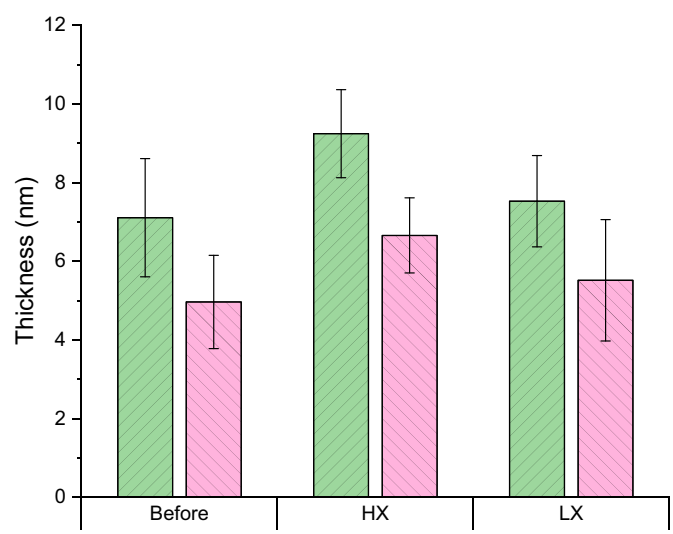

Fig. 5. Film thickness approximation of CNF (▨) and TCNF (▨) films determined from the QCM-D sensor resonance frequency difference in air.

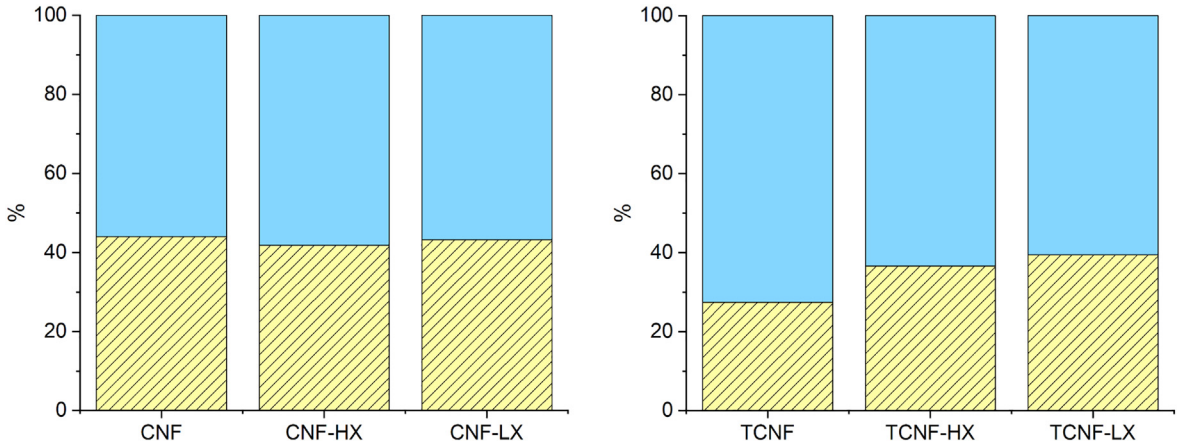

Fig. 6. Percentage of solid (▨) and water (▢) compositions of CNF film (left) and TCNF film (right). The film solid content was calculated using Sauerbrey equation [34] and the water amount was determined according to method by Kittle et al. [37].

As a result of adsorption of the HX on the CNF film, the amount of water in the film increased from the 56% to 58% and to 57% with LX adsorption. Similar increase in the amount of water in the CNF film was observed by comparing the QCM-D and SPR response. It enabled quantification of the water and indicated that the film of LX adsorbed on CNFs contained 0.59 mg/m^2 water and HX, 1.74 mg/m^2.

In the case of the TCNF film, the amount of water in the film decreased with both HX and LX adsorption from the 73% to 63% and 61%, respectively. Adsorption of uncharged polymers on charged surfaces leads to suppression of the electric double layer and can also be associated by movement of water. We hypothesize that the adsorbed oxidized xylan was able to replace water in the film resulting in the observed decrease in the amount of water in the films. Similar behavior did not take place with the neutral CNF film possibly because the film is less swollen than the adsorbate and hence the adsorption leads to increase in the water content.

While comparing the hydration of the films, one needs to bear in mind that since the TCNF films were thinner than the CNF films, but the LX adsorbed to CNFs and the HX and LX adsorbed to TCNFs with similar adsorbed mass on (Fig. 3), the ratio of the adsorbate to the film is higher in the case of the TCNFs. This can be a contributor in the more pronounced modulation of the hydration in the films. The difference in the solid matter to water ratio can be observed in Fig. 6.

Kontturi et al. [53] have reported that adsorption of cationic polyelectrolyte on nanocellulose films reduced the water content 10–20% while adsorption of anionic carboxymethyl cellulose led to swelling of the films and increased the retained water in the thin film with almost 50%. Here we see smaller changes, however, the molecular weight of the oxidized xylans (<10,000 g/mol) were much lower than those reported by Kontturi et al. (300,000 g/mol) [53]. Hence, we suggest that the molecular weight, adsorbed amount and charge in the system are intertwined factors that define the swelling and deswelling of cellulose thin film system and the increase in molecular weight of the xylan can be the next step towards valorization of wood xylans in the emerging materials.

4. Conclusions

The underutilized wood-xylans were rendered more water-soluble than the non-oxidized grades and could be adsorbed from aqueous conditions on neutral and negatively charged cellulose films. The adsorbed molecules reduced the amount of water in the charged films indicating that the oxidized xylan molecules have potential to reduce the swelling of the charged TCNF film. Furthermore, we conclude the following regarding fundamental characteristics of the xylans in solutions and at interfaces. The xylans were incorporated into films of CNFs via adsorption whose extent was found to be defined by molecular weight of the oxidized xylan and the cellulose film charge. The molecular weight was found to be the underlying factor to determine water-solubility and was indicated by that the d_H of the HX oxidized xylan was more sensitive to increase in concentration than the LX grade. We take the lower solubility as the reason for that the HX oxidized xylan adsorbed more on the cellulose substrate than did the LX grade. The adsorption of the HX grade was reduced on a negatively charged cellulose surface compared to the adsorption on the neutral surface indicating that the adsorption on the charged surface is governed by the electrostatic interactions as well. The assembly of these bio-based macromolecules at the water-rich cellulose interface is slow, which is due to the inherent polydispersity of the native molecules. The use of polymeric wood-xylans in materials engineering has been challenged by a lack in benefit in final product properties but also low water-solubility of the biomass molecules. Here we initiate endeavors of using oxidation for facilitating both solubility and providing functionality to xylans to valorize them in materials engineering.

CRediT authorship contribution statement

CP: Investigation, analysis, visualization, writing-reviewing and editing.
HA: Investigation, visualization, writing-reviewing and editing,
AS: Conceptualization, methodology, writing-reviewing and editing.
TN: Conceptualization, methodology, writing-reviewing and editing.

Acknowledgement

Swedish Research Council grant with registration number 2017-05138 and Wallenberg Wood Science Center are acknowledged for funding. Parveen Kumar Deralia and Joanna Wojtasz-Mucha for help with carbohydrate analysis. Division of Forest Products and Chemical Engineering at Chalmers is thanked for access to carbohydrate analysis. Gustav Ferrand-Drake Del Castillo for generous help with SPR. Chalmers Materials Analysis Laboratory is acknowledged for access to SPR.

Appendix A. Supplementary data

Supplementary data to this article can be found online at https://doi.org/10.1016/j.ijbiomac.2021.03.062.

References

[1] f. de Paula, C.B.C. de Paula, J. Contiero, Prospective biodegradable plastics from biomass conversion processes, Biofuels - State of development Edited by Krzysztof Biernat, IntechOpen, London, UK 2018, p. 247.

[2] D. Klemm, B. Philipp, T. Heinze, U. Heinze, W. Wagenknecht, Comprehensive Cellulose Chemistry. , Wiley, Weinheim, Germany, 1998.
[3] M.P. Arrieta, E. Fortunati, N. Burgos, M.A. Peltzer, J. López, L. Peponi, Nanocellulose-based polymeric blends for food packaging applications, in: D. Puglia, E. Fortunati, J.M. Kenny (Eds.), Multifunctional Polymeric Nanocomposites Based on Cellulosic Reinforcements, William Andrew Publishing 2016, pp. 205–252.
[4] M.A. Hubbe, A. Ferrer, P. Tyagi, Y. Yin, C. Salas, L. Pal, O.J. Rojas, Nanocellulose in thin films, coatings, and plies for packaging applications: a review, BioResources 12 (1) (2017) 2143–2233.
[5] H.M.C. Azeredo, M.F. Rosa, L.H.C. Mattoso, Nanocellulose in bio-based food packaging applications, Ind. Crop. Prod. 97 (2017) 664–671.
[6] W. Zhang, Y. Zhang, J. Cao, W. Jiang, Improving the performance of edible food packaging films by using nanocellulose as an additive, Int. J. Biol. Macromol. 166 (2021) 288–296.
[7] K. Jedvert, T. Heinze, Cellulose modification and shaping–a review, J. Polym. Eng. 37 (9) (2017) 845–860.
[8] M. Ek, G. Gellerstedt, G. Henriksson, Pulp and Paper Chemistry and Technology - Wood Chemistry and Biotechnology, 1, De Gruyter, Berlin, 2009.
[9] M. Pauly, S. Gille, L. Liu, N. Mansoori, A. de Souza, A. Schultink, G. Xiong, Hemicellulose biosynthesis, Planta 238 (4) (2013) 627–642.
[10] R.P. de Vries, J. Visser, Aspergillus enzymes involved in degradation of plant cell wall polysaccharides, Microbiol. Mol. Biol. Rev. 65 (4) (2001) 497–522.
[11] R. Tanaka, T. Saito, T. Hänninen, Y. Ono, M. Hakalahti, T. Tammelin, A. Isogai, Viscoelastic properties of core–shell-structured, hemicellulose-rich nanofibrillated cellulose in dispersion and wet-film states, Biomacromolecules 17 (6) (2016) 2104–2111.
[12] J. Stiernstedt, H. Brumer, Q. Zhou, T.T. Teeri, M.W. Rutland, Friction between cellulose surfaces and effect of xyloglucan adsorption, Biomacromolecules 7 (7) (2006) 2147–2153.
[13] L.C. Dalvi, C. Laine, T. Virtanen, T. Liitiä, T.-M. Tenhunen, H. Orelma, T. Tammelin, T. Tamminen, Study of xylan and cellulose interactions monitored with solid-state NMR and QCM-D, Holzforschung 74 (7) (2019) 643–653.
[14] Z. Jaafar, K. Mazeau, A. Boissiere, S. Le Gall, A. Villares, J. Vigouroux, N. Beury, C. Moreau, M. Lahaye, B. Cathala, Meaning of xylan acetylation on xylan-cellulose interactions: a quartz crystal microbalance with dissipation (QCM-D) and molecular dynamic study, Carbohydr. Polym. 226 (2019), 115315, .
[15] T. Köhnke, Å. Östlund, H. Brelid, Adsorption of arabinoxylan on cellulosic surfaces: influence of degree of substitution and substitution pattern on adsorption characteristics, Biomacromolecules 12 (7) (2011) 2633–2641.
[16] T. Köhnke, C. Pujolras, J.P. Roubroeks, P. Gatenholm, The effect of barley husk arabinoxylan adsorption on the properties of cellulose fibres, Cellulose 15 (4) (2008) 537–546.
[17] K.S. Mikkonen, L. Pitkänen, V. Liljeström, E.M. Bergström, R. Serimaa, L. Salmén, M. Tenkanen, Arabinoxylan structure affects the reinforcement of films by microfibrillated cellulose, Cellulose 19 (2) (2012) 467–480.
[18] T. Benselfelt, E.D. Cranston, S. Ondaral, E. Johansson, H. Brumer, M.W. Rutland, L. Wågberg, Adsorption of xyloglucan onto cellulose surfaces of different morphologies: an entropy-driven process, Biomacromolecules 17 (9) (2016) 2801–2811.
[19] M.A. Kabel, H. van den Borne, J.P. Vincken, A.G.J. Voragen, H.A. Schols, Structural differences of xylans affect their interaction with cellulose, Carbohydr. Polym. 69 (1) (2007) 94–105.
[20] Å. Henriksson, P. Gatenholm, Controlled assembly of glucuronoxylans onto cellulose fibres, Holzforschung 55 (5) (2001) 494–502.
[21] A. Paananen, M. Österberg, M. Rutland, T. Tammelin, T. Saarinen, K. Tappura, P. Stenius, Interaction between cellulose and xylan: An atomic force microscope and quartz crystal microbalance study, in: P. Gatenholm, M. Tenkanen (Eds.), Hemicelluloses: Science and Technology, 864, American Chemical Society 2003, pp. 269–290.
[22] M. Busse-Wicher, N.J. Grantham, J.J. Lyczakowski, N. Nikolovski, P. Dupree, Xylan decoration patterns and the plant secondary cell wall molecular architecture, Biochem. Soc. Trans. 44 (1) (2016) 74–78.
[23] T.J. Simmons, J.C. Mortimer, O.D. Bernardinelli, A.-C. Pöppler, S.P. Brown, E.R. deAzevedo, R. Dupree, P. Dupree, Folding of xylan onto cellulose fibrils in plant cell walls revealed by solid-state NMR, Nat. Commun. 7 (2016), 13902, .
[24] L. Falcoz-Vigne, Y. Ogawa, S. Molina-Boisseau, Y. Nishiyama, V. Meyer, M. Petit-Conil, K. Mazeau, L. Heux, Quantification of a tightly adsorbed monolayer of xylan on cellulose surface, Cellulose 24 (9) (2017) 3725–3739.
[25] Å. Linder, R. Bergman, A. Bodin, P. Gatenholm, Mechanism of assembly of xylan onto cellulose surfaces, Langmuir 19 (12) (2003) 5072–5077.
[26] C. Laine, A. Harlin, J. Hartman, S. Hyvärinen, K. Kammiovirta, B. Krogerus, H. Pajari, H. Rautkoski, H. Setälä, J. Sievänen, J. Uotila, M. Vähä-Nissi, Hydroxyalkylated xylans – their synthesis and application in coatings for packaging and paper, Ind. Crop. Prod. 44 (2013) 692–704.
[27] S. Kishani, F. Vilaplana, M. Ruda, P. Hansson, L. Wågberg, Influence of solubility on the adsorption of different xyloglucan fractions at cellulosewater interfaces, Biomacromolecules 21 (2) (2019) 772–782.
[28] Y.-C. Yang, X.-W. Mei, Y.-J. Hu, L.-Y. Su, J. Bian, M.-F. Li, F. Peng, R.-C. Sun, Fabrication of antimicrobial composite films based on xylan from pulping process for food packaging, Int. J. Biol. Macromol. 134 (2019) 122–130.
[29] M. Gröndahl, L. Eriksson, P. Gatenholm, Material properties of plasticized hardwood Xylans for potential application as oxygen barrier films, Biomacromolecules 5 (4) (2004) 1528–1535.
[30] H. Amer, T. Nypelö, I. Sulaeva, M. Bacher, U. Henniges, A. Potthast, T. Rosenau, Synthesis and characterization of periodate-oxidized polysaccharides: Dialdehyde xylan (DAX), Biomacromolecules 17 (9) (2016) 2972–2980.
[31] E. Maekawa, T. Kosaki, T. Koshijima, Periodate oxidation of mercerized cellulose and regenerated cellulose, Wood Res. Bull Wood Res. Inst. Kyoto Univ. 73 (1986) 44–49.
[32] T. Saito, S. Kimura, Y. Nishiyama, A. Isogai, Cellulose nanofibers prepared by TEMPO-mediated oxidation of native cellulose, Biomacromolecules 8 (8) (2007) 2485–2491.
[33] O. Theander, E.A. Westerlund, Studies on dietary fiber. 3. Improved procedures for analysis of dietary fiber, J. Agric. Food Chem. 34 (2) (1986) 330–336.
[34] T. Tammelin, R. Abburi, M. Gestranius, C. Laine, H. Setälä, M. Österberg, Correlation between cellulose thin film supramolecular structures and interactions with water, Soft Matter 11 (21) (2015) 4273–4282.
[35] A. Naderi, P.M. Claesson, Adsorption properties of polyelectrolyte— surfactant complexes on hydrophobic surfaces studied by QCM-D, Langmuir 22 (18) (2006) 7639–7645.
[36] D. Johannsmann, K. Mathauer, G. Wegner, W. Knoll, Viscoelastic properties of thin films probed with a quartz-crystal resonator, Phys. Rev. B 46 (12) (1992) 7808–7815.
[37] J.D. Kittle, X. Du, F. Jiang, C. Qian, T. Heinze, M. Roman, A.R. Esker, Equilibrium water contents of cellulose films determined via solvent exchange and quartz crystal microbalance with dissipation monitoring, Biomacromolecules 12 (8) (2011) 2881–2887.
[38] V.S. Craig, M. Plunkett, Determination of coupled solvent mass in quartz crystal microbalance measurements using deuterated solvents, J. Colloid Interface Sci. 262 (1) (2003) 126–129.
[39] J. Junesch, T. Sannomiya, A.B. Dahlin, Optical properties of nanohole arrays in metal–dielectric double films prepared by mask-on-metal colloidal lithography, ACS Nano 6 (11) (2012) 10405–10415.
[40] K.A. Kristiansen, A. Potthast, B.E. Christensen, Periodate oxidation of polysaccharides for modification of chemical and physical properties, Carbohydr. Res. 345 (10) (2010) 1264–1271.
[41] A.H. Pandit, N. Mazumdar, S. Ahmad, Periodate oxidized hyaluronic acid-based hydrogel scaffolds for tissue engineering applications, Int. J. Biol. Macromol. 137 (2019) 853–869.
[42] Y. Zuo, W. Liu, J. Xiao, X. Zhao, Y. Zhu, Y. Wu, Preparation and characterization of dialdehyde starch by one-step acid hydrolysis and oxidation, Int. J. Biol. Macromol. 103 (2017) 1257–1264.
[43] M. Börjesson, A. Larsson, G. Westman, A. Ström, Periodate oxidation of xylan-based hemicelluloses and its effect on their thermal properties, Carbohydr. Polym. 202 (2018) 280–287.
[44] G.-Q. Fu, S.-C. Zhang, G.-G. Chen, X. Hao, J. Bian, F. Peng, Xylan-based hydrogels for potential skin care application, Int. J. Biol. Macromol. 158 (2020) 244–250.
[45] S. Koprivica, M. Siller, T. Hosoya, W. Roggenstein, T. Rosenau, A. Potthast, Regeneration of aqueous periodate solutions by ozone treatment: a sustainable approach for dialdehyde cellulose production, ChemSusChem 9 (8) (2016) 825–833.
[46] H. Liimatainen, J. Sirviö, H. Pajari, O. Hormi, J. Niinimäki, Regeneration and recycling of aqueous periodate solution in dialdehyde cellulose production, J. Wood Chem. Technol. 33 (4) (2013) 258–266.
[47] T. Nypelö, B. Berke, S. Spirk, J.A. Sirviö, Review: periodate oxidation of wood polysaccharides-modulation of hierarchies, Carbohydr. Polym. 252 (2021), 117105, .
[48] S.F. Plappert, S. Quraishi, N. Pircher, K.S. Mikkonen, S. Veigel, K.M. Klinger, A. Potthast, T. Rosenau, F.W. Liebner, Transparent, flexible, and strong 2,3-dialdehyde cellulose films with high oxygen barrier properties, Biomacromolecules 19 (7) (2018) 2969–2978.
[49] F. Jiang, Y.-L. Hsieh, Self-assembling of TEMPO oxidized cellulose nanofibrils as affected by protonation of surface carboxyls and drying methods, ACS Sustain. Chem. Eng. 4 (3) (2016) 1041–1049.
[50] A.B. Fall, S.B. Lindström, O. Sundman, L. Ödberg, L. Wågberg, Colloidal stability of aqueous nanofibrillated cellulose dispersions, Langmuir 27 (18) (2011) 11332–11338.
[51] P. Eronen, M. Österberg, S. Heikkinen, M. Tenkanen, J. Laine, Interactions of structurally different hemicelluloses with nanofibrillar cellulose, Carbohydr. Polym. 86 (3) (2011) 1281–1290.
[52] C. Chang, M. He, J. Zhou, L. Zhang, Swelling behaviors of pH- and salt-responsive cellulose-based hydrogels, Macromolecules 44 (6) (2011) 1642–1648.
[53] K.S. Kontturi, E. Kontturi, J. Laine, Specific water uptake of thin films from nanofibrillar cellulose, J. Mater. Chem. A 1 (43) (2013) 13655–13663.
[54] G.J. Fleer, M.A. Cohen Stuart, J.M.H.M Scheutjens, T. Cosgrove, B. Vincent, Polymers at Interfaces. , Chapman & Hall, London, UK, 1993.